



Bioresorbable glass effect on the physico-chemical properties of bilayered scaffolds for osteochondral regeneration

Piergiorgio Gentile^a, Valeria Chiono^a, Chiara Tonda-Turo^a, Clara Mattu^a, Francesco Baino^b, Chiara Vitale-Brovarone^b, Gianluca Ciardelli^{a,c,*}

^a Mechanical and Aerospace Engineering Department, Politecnico di Torino, Corso Duca degli Abruzzi 24, 10129 Turin, Italy

^b Institute of Materials Engineering and Physics, Applied Science and Technology Department, Politecnico di Torino, Corso Duca degli Abruzzi 24, 10129 Turin, Italy

^c CNR-IPCF UOS-Pisa, Via Moruzzi 1, 56124 Pisa, Italy

ARTICLE INFO

Article history:

Received 14 May 2012

Accepted 7 August 2012

Available online 17 August 2012

Keywords:

Composite scaffolds

Bilayered

Bioresorbable glass

Gelatin

Osteochondral bone

ABSTRACT

In this work, bilayered and bioresorbable composite scaffolds are developed with mechanical and functional properties for osteochondral tissue engineering. Porous scaffolds made of gelatin (G) and bioresorbable phosphate glass (I-CEL2) with different compositions (I-CEL2/G 0/100; 30/70; 70/30 %w/w) were fabricated by freeze-drying. Samples were crosslinked using γ -glycidoxypropyltrimethoxysilane to improve mechanical strength and thermal stability. I-CEL2/G samples showed interconnected pores having an average diameter ranging from $139 \pm 5 \mu\text{m}$ for I-CEL2/G 0/100 to $116 \pm 9 \mu\text{m}$ for I-CEL2/G 70/30. GPTMS-crosslinking and the increase of I-CEL2 amount stabilized the composites to water solution, as shown by swelling tests. The compressive modulus increased by increasing I-CEL2 amount up to $7.6 \pm 0.5 \text{ MPa}$ for I-CEL2/G 70/30.

© 2012 Elsevier B.V. All rights reserved.

1. Introduction

Osteochondral defects are focal areas where cartilage damage and injury of the adjacent subchondral bone takes place, that can be treated using different strategies, such as (i) osteochondral autograft [1], (ii) autologous chondrocytes [2] or (iii) matrix-induced autologous chondrocyte implantation [3]. Nowadays, no successful method for complete regeneration of osteochondral defects exists [4]. A graft designed for treating large osteochondral defects should be a tissue-engineered osteochondral (bone–cartilage) composite (with a predefined size and shape) characterised by mechanical stability and an appropriate post-operative functionality under physiological conditions [5], to achieve simultaneous regeneration of both cartilage and subchondral bone. Bilayered scaffolds are proposed for repairing osteochondral defects, in order to allow the preparation of optimized different layers able to mimic the native extracellular matrix for each tissue type (bone and cartilage), tuning the physico-chemical, structural, and mechanical properties in a single structure [6]. Bilayered scaffolds have been classified into three types: (i) “Cartilage tissue on bone scaffold” in which chondrocytes or neocartilage tissue are seeded directly onto a

bone scaffold, (ii) “Assembled bilayered scaffolds” in which two distinct and different cartilage and bone scaffolds are assembled together before or during surgical implantation, and (iii) “Integrated bilayered scaffolds”, consisting of two different structures that are joined together through the integration of a material contained in both layers [7].

The potential advantages of glass/polymer composite scaffolds for regenerative medicine have been widely emphasized in the recent literature [8–10]. In this work, innovative bilayered sponge-like scaffolds, based on a bioresorbable phosphate glass and a glycidoxypropyltrimethoxysilane-crosslinked network of gelatin (G) were studied in order to investigate their potential for osteochondral tissue regeneration. The proposed matrices represent a new category of bilayered scaffolds, that could be easily obtained by a single step procedure.

2. Materials and methods

2.1. Scaffolds preparation

G (type A from porcine skin) and GPTMS were supplied from Sigma-Aldrich, Milan. Powders (particle size $< 30 \mu\text{m}$) of resorbable phosphate glass (I-CEL2; molar composition: 45% P_2O_5 , 3% SiO_2 , 26% CaO , 7% MgO , 15% Na_2O , 4% K_2O) were prepared as reported elsewhere [11–13]. The scaffolds were prepared according to the following procedures: G was dissolved in demineralised water at $50 \text{ }^\circ\text{C}$ to obtain a 2.5%(w/v) solution. I-CEL2 was added

* Corresponding author at: Mechanical and Aerospace Engineering Department, Politecnico di Torino, Corso Duca degli Abruzzi 24, 10129 Turin, Italy.
Tel.: +39 11 5646919; fax: +39 11 5646999.

E-mail address: gianluca.ciardelli@polito.it (G. Ciardelli).

to the gelatin solution to obtain I-CEL2/G composites with various weight ratios between the components: 0/100;30/70;70/30 (%w/w). The composites were coded as follows: I-CEL2/G 0/100;30/70;70/30. Then, GPTMS was added to the G solution as previously described [14]. The solutions were poured into polystyrene 24-multiwell containers for 24 h to complete the cross-linking reaction, and then freeze-dried (Scanvac-CoolSafe) at $-20\text{ }^{\circ}\text{C}$ for 48 h. Uncrosslinked sponges were prepared as control.

2.2. Scaffold characterization

The swelling behaviour was evaluated at $37\text{ }^{\circ}\text{C}$ using a phosphate buffered saline at pH 7.4 (Sigma-Aldrich). The swelling degree was measured after 3, 6 and 24 h and calculated as: $\Delta W_s(\%) = ((W_s - W_0)/W_0) \times 100$, where W_0 and W_s are the sample weights before and after swelling, respectively.

Morphological (SEM, Philips 525 M) and compositional analysis (energy-dispersive spectroscopy, EDS; Philips EDAX 9100) were performed on fractured specimen sections. The samples were sputter coated with carbon prior to the examination.

Pore dimension and distribution was quantified by micro-computed tomography (μ -CT, MicroXCT200 series, XRADIA). No contrasting agent was added and the samples had a minimum size of $1 \times 1 \times 0.5\text{ mm}^3$. The scanner was set at a voltage of 40 kV; the samples were scanned at $0.597\text{ }\mu\text{m}$ pixel resolution by 1000 slices covering the sample height.

Compressive stress–strain curves were measured using MTS QTest/10 device and a load cell of 50 N. Test specimens ($n=3$) were cylinder-shaped sponges (1.2 cm diameter and an average height of 1.2 cm). The cross-head speed was set at 0.01 mm s^{-1} and the load was applied until the specimen was compressed to 70% of its original length. Young's modulus (E), collapse strength and strain (σ^* and ε^*) and collapse modulus (E^*) were measured from the stress–strain curves. E is the linear elastic regime slope, E^* is the collapse regime slope, σ^* and ε^* are, respectively, the stress and strain of transition from linear to collapse regime [15].

Calorimetric measurements were performed using TA-INSTRUMENTS DSC/Q20. The samples (6–8 mg) were hermetically sealed in aluminium pans. Heating was carried out at $10\text{ }^{\circ}\text{C min}^{-1}$ in the $30\text{--}130\text{ }^{\circ}\text{C}$ temperature range. Denaturation temperature (T_d) and enthalpy (ΔH_d) were calculated as the temperature of the maximum value of the denaturation endotherm and the peak area. Denaturation enthalpy was normalised with respect to G content.

3. Results and discussion

SEM analysis was performed to evaluate the effect of composition on scaffold morphology. Fig. 1(A) shows the typical foam-like morphology with interconnected pores of I-CEL2/G 0/100 scaffold. EDS spectra of pure G scaffold (insert in Fig. 1(A)) indicates the presence of the characteristic elements contained in gelatin: carbon(C), nitrogen(N) and oxygen(O). Fig. 1(B) and (C) show I-CEL2/G 30/70 and I-CEL2/G 70/30 scaffolds: EDS analysis demonstrated that these samples were characterized by a typical bilayered structure, consisting of a top gelatin layer and a bottom layer mainly constituted of I-CEL2 and a very low gelatin amount. EDS spectra of the bottom layers showed the characteristic elements of I-CEL2, namely silicon(Si), potassium(K), sodium(Na), magnesium(Mg), calcium(Ca) and phosphorus(P) (insert in Fig. 1(B) and (C)) where EDS spectra of the top layers showed the characteristic elements of gelatin. The porosity degree was different in the top and in the bottom layers, and dependent on the concentration of I-CEL2. In particular, the gelatin top layer exhibited a total porosity of 86.2 vol%; on the other hand, the

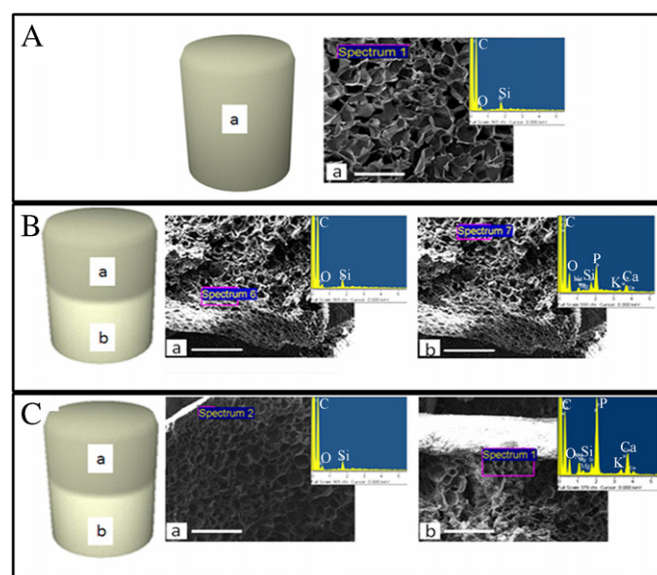


Fig. 1. SEM micrographs and EDS spectra of I-CEL2/G composite scaffolds: (A) I-CEL2/G 0/100, (B) I-CEL2/G 30/70, (C) I-CEL2/G 70/30 (bar: 100 μm). For each SEM micrographs (a) indicates the top side, and (b) the bottom side.

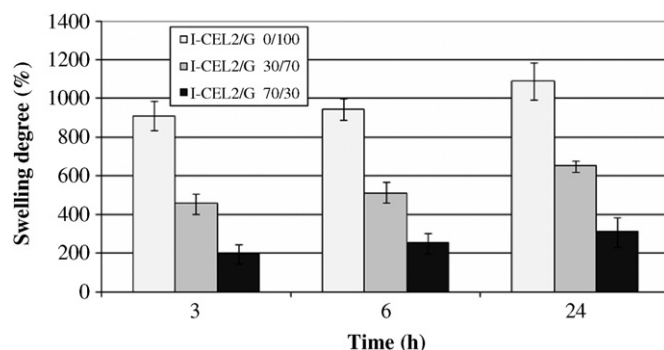


Fig. 2. Swelling behavior of scaffolds as a function of time.

porosity degree of the bottom layer was found to vary from 67.1 to 86.2 vol% with decreasing of the concentration of I-CEL2. The dependence of porosity degree on I-CEL2 amount has to be ascribed to the deposition of the bioresorbable glass particles on the pore walls as confirmed subsequently by SEM examination (Fig. 1(B) and (C)). The mean pore size of I-CEL2/G 0/100 and of the top layers of I-CEL2/G 30/70 and I-CEL2/G 70/30 scaffolds was found to be around $149.2\text{ }\mu\text{m}$; on the other hand, the mean pore size of the bottom layers was found to vary from $135.7\text{ }\mu\text{m}$ for I-CEL2/G 30/70 to $126.5\text{ }\mu\text{m}$ for I-CEL2/G 70/30 composites, which demonstrates that the average pore size decreased with increasing I-CEL2 content. All samples showed a high interconnected network of pores (95%) with higher size than $95.1\text{ }\mu\text{m}$, as assessed by μ -CT analysis.

Different methods were reported in literature to prepare bilayered scaffolds [16–19], generally based on two consecutive different procedures (e.g., sintering and freeze-drying). In our case, bilayered scaffolds could be easily obtained by casting I-CEL2/G mixture solutions: the higher density of I-CEL2 (2.6 g/cm^3) as compared to the G phase caused the progressive precipitation of I-CEL2 at the bottom of multiwell containers for gravity when the solution was poured into polystyrene 24-multiwell containers for 24 h to complete the crosslinking reaction.

The increase in swelling also allows the scaffold to avail nutrients from culture media more effectively [20]. Fig. 2 reports

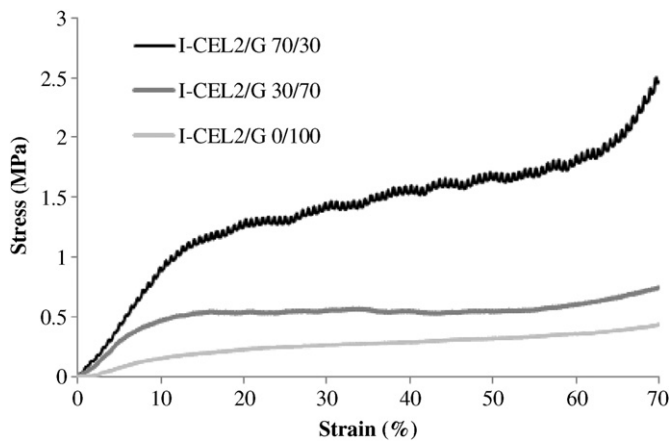


Fig. 3. Stress–strain curves of the porous scaffolds compressed at a strain of (0–70%).

Table 1

Elastic modulus, collapse strength and strain, and collapse modulus calculated from the corresponding stress–strain curves.

I-CEL2/G sample	E (MPa)	σ^* (MPa)	ε^* (%)	$\Delta\sigma/\Delta\varepsilon$ (kPa)
0/100	1.9 ± 0.2	0.27 ± 0.04	14.4 ± 1.5	0.09 ± 0.01
30/70	5.6 ± 0.4	0.56 ± 0.02	10.0 ± 0.3	0.13 ± 0.03
70/30	7.6 ± 0.5	0.63 ± 0.13	8.3 ± 0.6	1.26 ± 0.02

the swelling degree as a function of time for composite porous matrices with different compositions. All composites showed a similar swelling behaviour: the swelling degree slightly increased over time from 3 to 24 h. I-CEL2/G 0/100 scaffolds displayed the highest swelling at each time interval (from $909 \pm 52\%$ at 3 h to $1088 \pm 60\%$ at 24 h). For I-CEL2/G 30/70 samples, at 3 h the swelling degree was about $457 \pm 50\%$. At 12 h the swelling degree did not increase significantly, while at 24 h the swelling ratio was about $650 \pm 45\%$. Moreover, for I-CEL2/G 70/30 composites, swelling ratio was about $197 \pm 53\%$ after 3 h, while at 6 and 24 h, the swelling degree did not increase significantly. At each time, swelling degree was found to decrease with increasing I-CEL2 amount, because of the lower hydrophilicity of the inorganic phase as compared to the polymeric matrix causing a decrease of the water sorption as suggested in previous works [21,22].

Fig. 3 shows the stress–strain curves obtained for the matrices by compression tests. A significant increase of compression Young's modulus was obtained by adding I-CEL2 into the gelatin matrix, due to the superior stiffness of the inorganic phase. compression behaviour of the glass as compared to G phase (1.9 ± 0.2 MPa for I-CEL2/G 0/100 up to 7.6 ± 0.5 MPa for I-CEL2/G 70/30). As shown in Table 1, the collapse strength and collapse strain were characterized by a different trend as a function of the I-CEL2 amount. In particular, the increase of the inorganic phase caused a progressive, slight decrease in the deformability of the composite scaffold and an increase of the collapse strength and modulus.

DSC analysis was performed to analyse the thermal behaviour of scaffolds as a function of composition together with the influence of I-CEL2 on gelatin thermal properties. Crosslinking increased the thermal stability of gelatin helices as shown by the shift of the T_d to higher values (95.1°C for I-CEL2/G 0/100) as compared to uncrosslinked gelatin scaffolds (92.3°C) [19]. Crosslinking generally induced a decrease in the denaturation enthalpy, which was ascribed both to a reduction of hydrogen bonds, and to a simultaneous increase in the extent of covalent crosslinks [23] (30.2 J g^{-1} for uncrosslinked gelatin and 26.0 J g^{-1}

for I-CEL2/G 0/100). The denaturation temperature of I-CEL2/G composites with different weight ratios between inorganic and organic phase slightly increased with respect to pure crosslinked gelatin film (97.0°C for I-CEL2/G 30/70 and 98.5°C for I-CEL2/G 70/30). It is worth noting that the composites showed low denaturation enthalpy values (7.1 J g^{-1} for I-CEL2/G 30/70 and 5.2 J g^{-1} for I-CEL2/G 70/30), probably due to a reduction of the helical structure as a consequence of the strong interactions between bioresorbable glass and gelatin.

4. Conclusions

A new category of bilayered scaffolds were successfully and easily prepared by a single step procedure for osteochondral tissue regeneration. The obtained scaffolds showed an interconnected network of macropores with $100\text{--}150\text{ }\mu\text{m}$ average size as shown by SEM and $\mu\text{-CT}$ analysis. Moreover, scaffolds containing I-CEL2 were particularly interesting due to their (i) increased stability in aqueous solution as evidenced by swelling tests, (ii) increased compressive Young's modulus with respect to the pure G, and (iii) interactions between the phases as suggested by the slight increase in the denaturation temperature. The obtained composites represent promising candidates for future trials in the field of osteochondral regeneration. Additional work is in progress, with the aim to investigate the biocompatibility of these composite scaffolds, in vitro and in vivo.

Acknowledgements

The work was funded by Italian Ministry of University and Research for P. Gentile's Ph.D. Grant.

References

- Marcacci M, Kon E, Delcogliano M, Filardo G, Busacca M, Zaffagnini S. *Am J Sports Med* 2007;35:2014–21.
- Lee CY, Liu X, Hsu HC, Wang DY, Luo ZP. *Connect Tissue Res* 2005;46:93–9.
- Ait Si, Selmi T, Neyret P, Verdonk PCM, Barnouin L. *Tech Knee Surg* 2007;6:253–8.
- Swieszkowski W, Tuan BH, Kurzydowski KJ, Huttmacher DW. *Biomol Eng* 2007;24(5):489–95.
- Schaefer D, Martin I, Jundt G, Seidel J, Heberer M, Grodzinsky A, et al. *Arthritis Rheum* 2002;46:2524–34.
- Malafaya PB, Reis RL. *Acta Biomater* 2009;5:644–50.
- O'Shea TM, Miao X. *Tissue Eng B* 2008;14:447–64.
- Rezwan K, Chen QZ, Blaker JJ, Boccaccini AR. *Biomaterials* 2006;27:3413–31.
- Yunos DM, Bretcanu O, Boccaccini AR. *J Mater Sci* 2008;43:4433–42.
- Ahmed I, Jones IA, Parsons AJ, Bernard J, Farmer J, Scotchford CA, et al. *J Mater Sci: Mater Med* 2011;22:1825–34.
- Leonardi E, Ciapetti G, Baldini N, Novajra G, Verné E, Baino F, et al. *Acta Biomater* 2010;6:598–606.
- Vitale-Brovarone C, Baino F, Bretcanu O, Verné E. *J Mater Sci: Mater Med* 2009;20:2197–205.
- Vitale-Brovarone C, Ciapetti G, Leonardi E, Baldini N, Bretcanu O, Verné E, et al. *J Biomater Appl* 2011;26:465–89.
- Tonda-Turo C, Gentile P, Saracino S, Chiono V, Nandagiri VK, Muzio G, et al. *Int J Biol Macromol* 2011;49:700–6.
- Kanungo BP, Silva E, Van Vliet K, Gibson LJ, et al. *Acta Biomater* 2008;4:490–503.
- Olivera JM, Rodrigues MT, Silva SS, Malafaya PB, Gomes ME, Viegas CA, et al. *Biomaterials* 2006;27:6123–37.
- Chen J, Chen H, Li P, Diao H, Zhu S, Dong L, et al. *Biomaterials* 2011;32:4793–805.
- Tampieri A, Sandri M, Landi E, Pressato D, Francioli S, Quarto R, et al. *Biomaterials* 2008;29:3539–46.
- Keeney M, Pandit A. *Tissue Eng B* 2009;15:55–73.
- Janaki K, Elamathi S, Sangeetha D, et al. *Trends Biomater Artif Organs* 2008;22:169–78.
- Ciardelli G, Gentile P, Chiono V, Mattioli-Belmonte M, Vozzi G, Barbani N, et al. *J Biomed Mater Res Part A* 2010;92:137–51.
- Gentile P, Chiono V, Boccafocchi F, Baino F, Vitale-Brovarone C, Verné E, et al. *J Biomater Sci, Polym Ed* 2010;21:1207–26.
- Bigi A, Cojazzi G, Panzavolta S, Rubini K, Roveri N. *Biomaterials* 2001;20:763–8.